Supplement of Atmos. Chem. Phys., 24, 2607–2624, 2024
https://doi.org/10.5194/acp-24-2607-2024-supplement

Atmospheric Chemistry and Physics
Open Access

Supplement of

Variation in chemical composition and volatility of oxygenated organic aerosol in different rural, urban, and mountain environments

Wei Huang et al.

Correspondence to: Claudia Mohr (claudia.mohr@psi.ch)

Table S1. Campaign-average (average ± 1 standard deviation) parameters for meteorology, trace gases, equivalent black carbon (eBC), total organics and total $PM_{2.5}$, double bond equivalent (DBE) values, and number of carbon atoms (nC) and oxygen atoms (nO) at different locations and different seasons.

Name	*T* (°C)	RH (%)	O_3 (ppbv)	NO_2 (ppbv)	SO_2 (ppbv)	eBC (μg m^{-3})	Org[a] (μg m^{-3})	$PM_{2.5}$[a] (μg m^{-3})	DBE	nC	nO	$\log_{10}C_{sat}$ (298K) (μg m^{-3})	$\log_{10}C_{sat}$ (*T*) (μg m^{-3})
MCC-t	0.3±2.1	53.0±22.4	/	/	/	0.2±0.4	0.3±0.5	1.0±1.8	3.1±0.2	8.4±0.8	6.2±0.3	1.6±0.3	-0.2±0.4
MCC-d	-0.4±1.9	52.2±18.8	/	/	/	0.3±0.4	0.5±0.5	1.6±1.4	3.2±0.1	7.7±0.7	5.8±0.3	2.2±0.4	0.6±0.3
REL	19.9±3.9	76.1±15.2	22.7±12.4	11.3±5.2	1.4±1.0	0.7±0.4	3.7±2.1	6.6±4.2	3.1±0.1	9.2±0.8	6.6±0.5	1.0±0.6	0.7±0.7
RAB	24.2±3.2	83.1±15.2	25.0±12.5	0.6±0.6	0.2±0.4	/	4.1±2.5	6.0±3.2	2.9±0.1	8.0±0.4	5.7±0.2	2.0±0.2	2.0±0.3
RHT	8.1±6.1	66.0±23.7	36.1±10.1	0.4±0.6	0.2±0.2	0.1±0.2	1.6±2.0	2.3±2.3	3.1±0.1	9.1±0.6	5.7±0.3	2.2±0.2	1.0±0.4
UST-s	24.6±4.0	55.1±12.8	29.6±7.5	9.7±4.1	3.9±2.8	1.0±0.3	5.1±3.2	7.1±3.3	3.4±0.1	8.8±0.4	6.4±0.2	1.6±0.2	1.6±0.3
UST-w	2.0±3.7	61.4±10.1	17.1±8.7	15.8±3.9	1.4±0.8	1.2±0.1	8.4±5.6	27.0±11.9	3.4±0.1	8.7±0.9	6.7±0.2	1.3±0.4	-0.4±0.4
UKA-s	25.9±6.6	49.8±21.0	37.4±19.8	9.6±6.4	/	0.7±0.4	3.9±2.4	5.9±2.8	3.6±0.2	10.7±0.8	7.0±0.4	0.8±0.6	0.6±0.8
UKA-w	13.2±3.3	56.4±13.4	27.8±10.0	9.2±7.1	0.6±1.0	0.5±0.5	1.9±1.6	3.9±3.6	3.5±0.1	11.2±0.8	7.1±0.4	0.4±0.5	-0.5±0.7
UDL	16.8±4.1	73.3±16.7	11.1±13.3	34.6±22.0	/	16.1±13.3	86.4±66.7	172.7±103.8	4.0±0.2	9.4±0.4	4.9±0.1	2.8±0.2	2.4±0.2

[a]Data were total non-refractory mass concentration from a high-resolution time-of-flight aerosol mass spectrometer (HR-ToF-AMS, Aerodyne Research Inc.) or an aerosol chemical speciation monitor (ACSM, Aerodyne Research Inc.).

Table S2. Deposition parameters and instrumental parameters at different locations and different seasons.

Name	Total inlet flow (L/min)/ Residence time (s)	Deposition time (min)	Mass loading (μg)[c]	FIGAERO type/ Sample mode	IMR body T (°C)	IMR pressure (mbar)	Ion source	Ratio of sample flow : ionizer flow	Ramp rate (°C/min)
MCC-t	7.0/1.4	120	0.3±0.3	Aerodyne/online	45	100	Corona discharge	2:1.3	13.3
MCC-d	7.0/1.4	120	0.4±0.4	Aerodyne/online	45	480	X-ray	2:1.3	13.3
REL	8.6/1.2	30	1.0±0.7	Aerodyne/online	45	100	Po-210	2:2	13.3
RAB	22/3.6	20	1.8±1.3	UW/online[d]	25	100	Po-210	2:2	10.0
RHT	11/4.2	30	0.5±0.8	UW/online[d]	25	100	Po-210	2:2	10.0
UST-s	8.7/0.8	112±43[b]	3.5±1.4	Aerodyne/offline	45	100	Po-210	2:2	13.3
UST-w	10.0/0.7	86±70[b]	4.0±1.0	Aerodyne/offline	45	100	Po-210	2:2	13.3
UKA-s	6.4/0.8	128±99[b]	3.2±2.1	Aerodyne/offline	45	100	Po-210	2:2	13.3
UKA-w	6.4/0.8	245±124[b]	3.0±1.5	Aerodyne/offline	45	100	Po-210	2:2	13.3
UDL	2.4[a]/2.8	3±1	0.6±0.5	Aerodyne/online	25	250	X-ray	2:1.5	6.7

[a]Average inlet flow of 3.5 L/min for the 1st week and 2 L/min for the next 2.5 weeks.

[b]Deposition time was average ± 1 standard deviation from offline filters.

[c]Mass loadings were calculated based on concurrent HR-ToF-AMS or ACSM measurements.

[d]FIGAERO inlet from the University of Washington, U.S., designed by Lopez-Hilfiker et al. (2014).

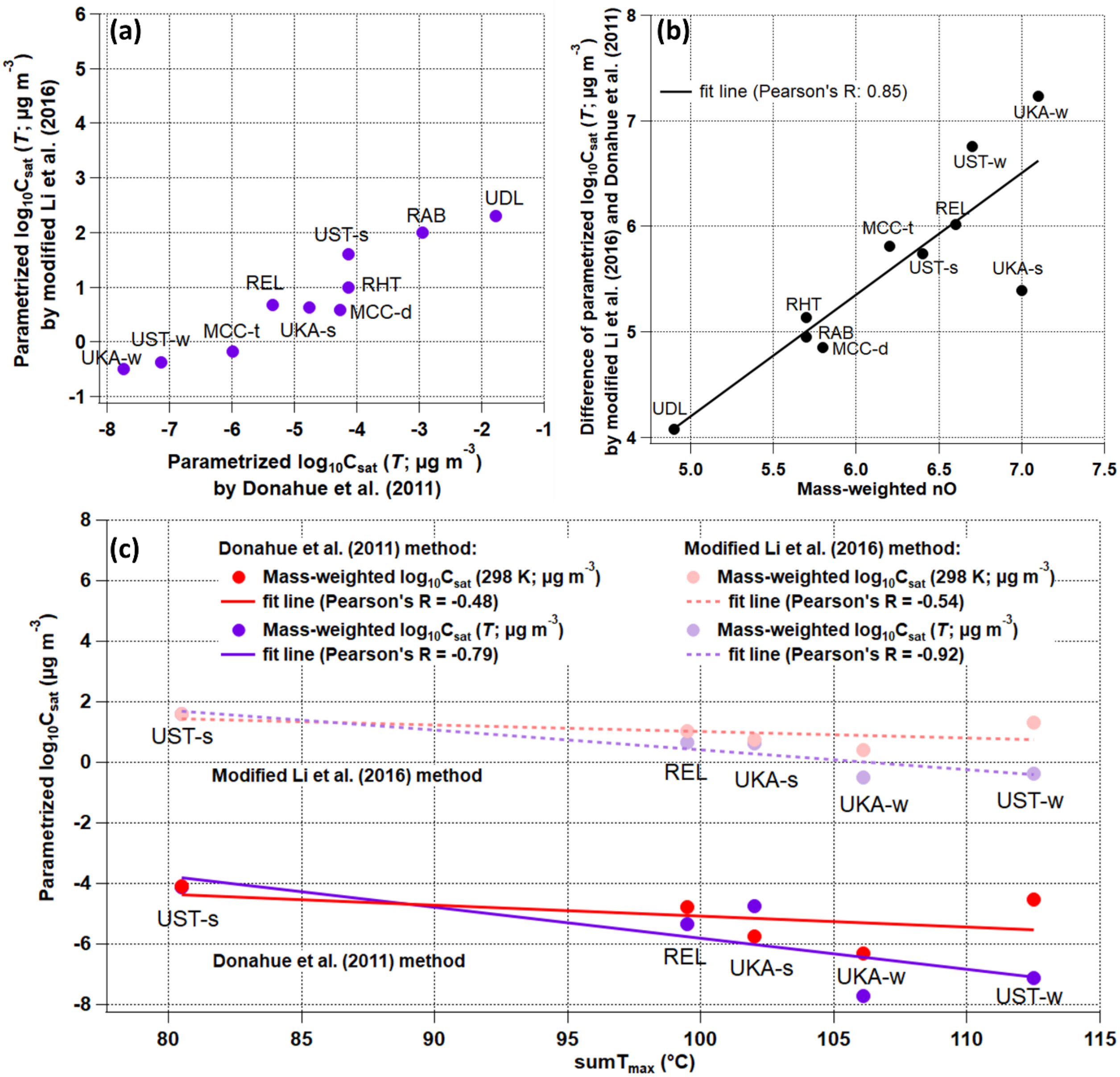

Figure S1. (a) Comparison of the campaign-average mass-weighted $\log_{10}C_{sat}$ (T) values using the modified Li et al. (2016) parametrization method (Daumit et al., 2013;Isaacman-VanWertz and Aumont, 2021) and the Donahue et al. (2011) method. **(b)** Comparison of the difference of campaign-average mass-weighted $\log_{10}C_{sat}$ (T) values using the modified Li et al. (2016) parametrization method (Daumit et al., 2013;Isaacman-VanWertz and Aumont, 2021) and the Donahue et al. (2011) method with the mass-weighted number of oxygen atoms (nO). **(c)** Comparison of the campaign-average mass-weighted $\log_{10}C_{sat}$ values and $sumT_{max}$ values for different locations and seasons (only datasets where the exact same FIGAERO setup was used), with mass-weighted $\log_{10}C_{sat}$ (298 K) in red and mass-weighted $\log_{10}C_{sat}$ (T) in purple; the colored lines are the fit lines for the corresponding markers.

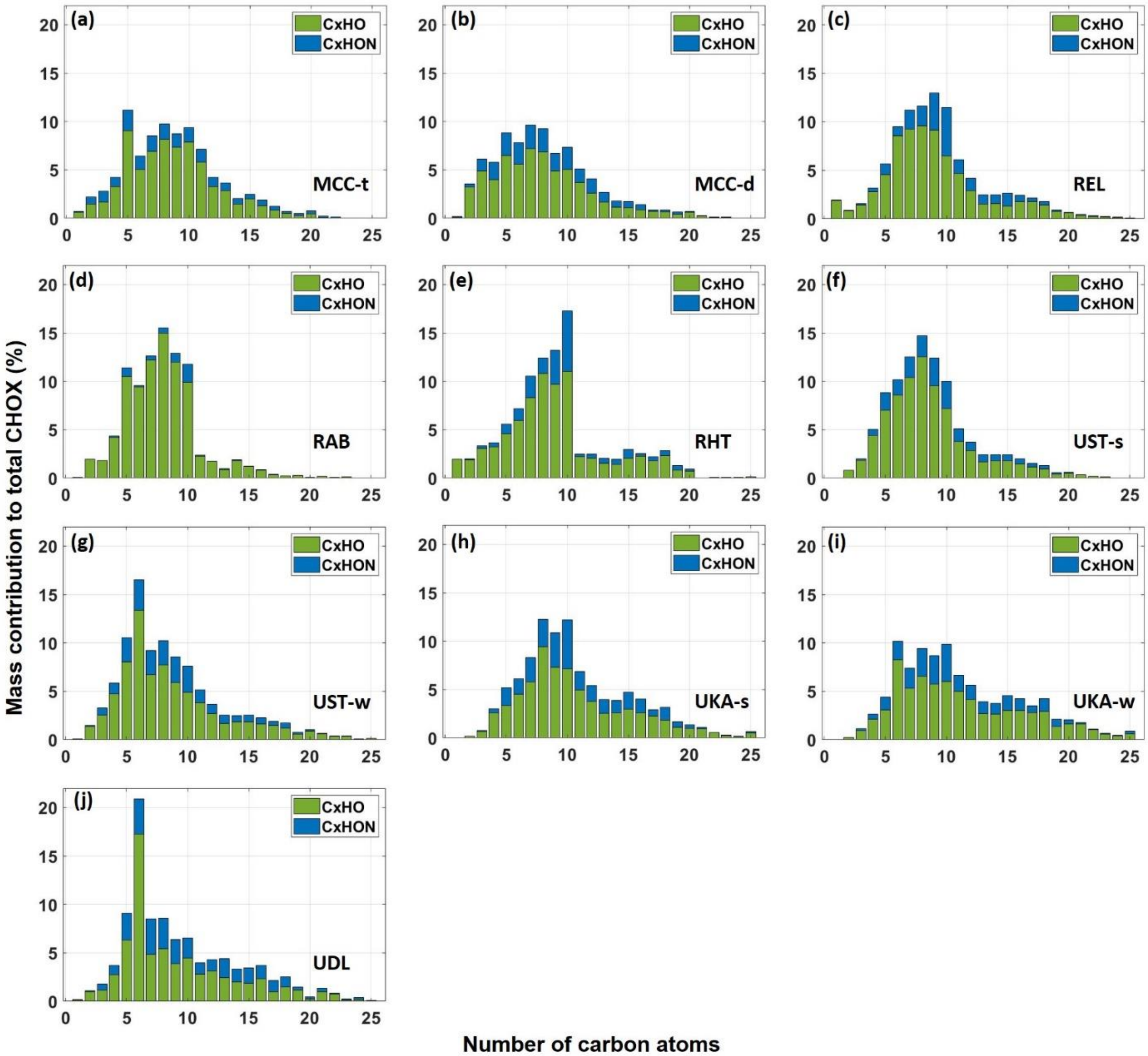

Figure S2. Mass contributions of CHO and CHON compounds to total CHOX compounds as a function of the number of carbon atoms for MCC-t (a), MCC-d (b), REL (c), RAB (d), RHT (e), UST-s (f), UST-w (g), UKA-s (h), UKA-w (i), and UDL (j).

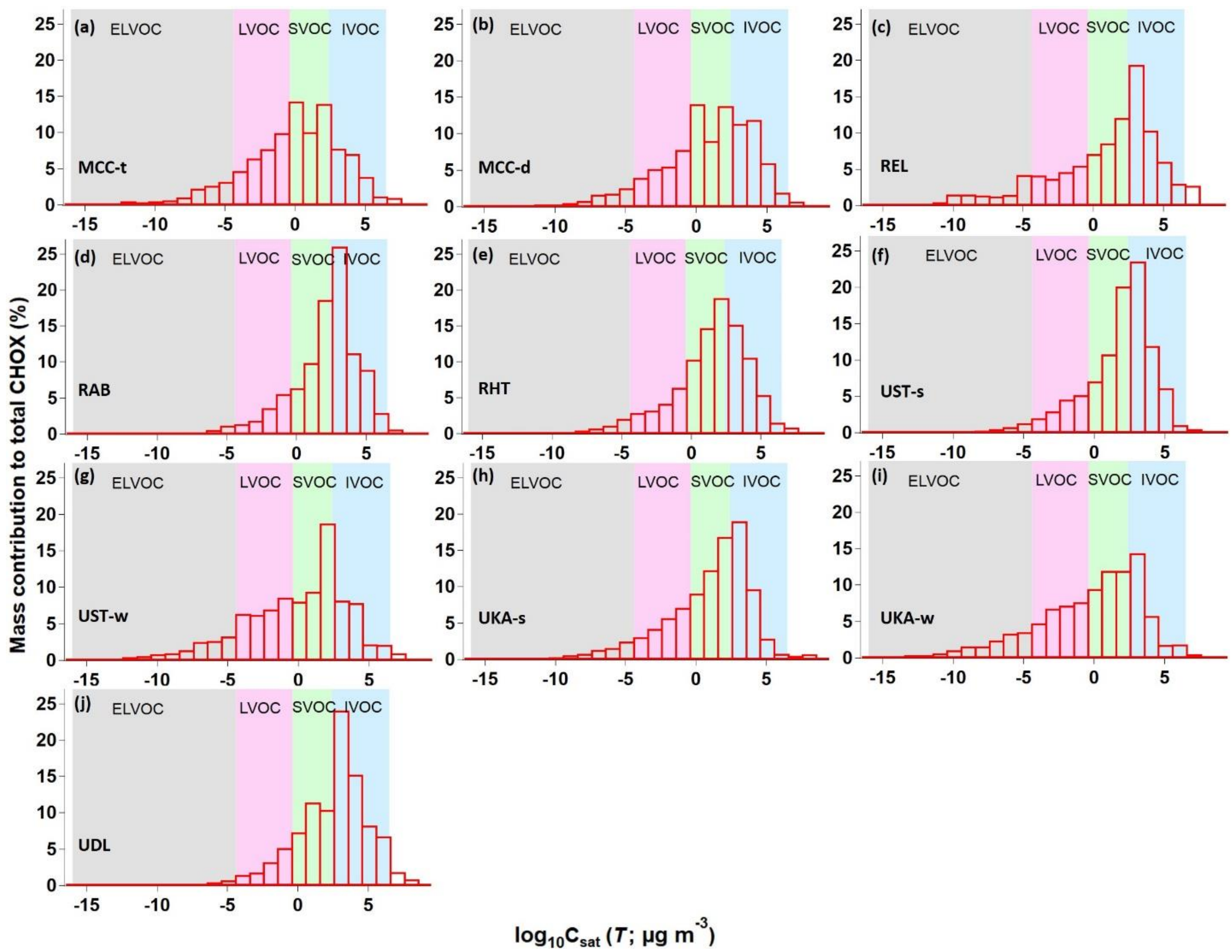

Figure S3. Volatility distribution for MCC-t (a), MCC-d (b), REL (c), RAB (d), RHT (e), UST-s (f), UST-w (g), UKA-s (h), UKA-w (i), and UDL (j) with the modified Li et al. (2016) parameterization method (Daumit et al., 2013;Isaacman-VanWertz and Aumont, 2021).

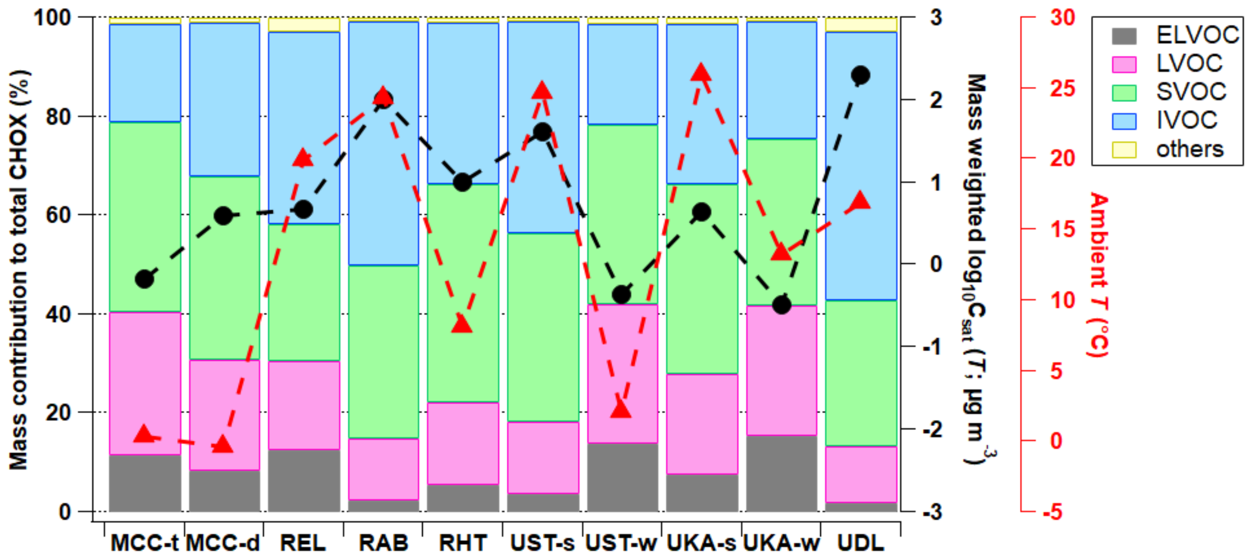

Figure S4. Comparison between ambient temperature (*T*) and campaign-average contribution (%) of different volatility groups resulting from VBS calculations to total organics (colored in bars) and campaign-average mass weighted $\log_{10}C_{sat}$ (*T*) values (in black markers) for different campaigns with the modified Li et al. (2016) parameterization method (Daumit et al., 2013;Isaacman-VanWertz and Aumont, 2021) (same as Figure 2). Compounds more volatile than IVOC with C_{sat} higher than $10^{6.5}$ μg m^{-3} (labelled as "others") contributed negligibly (0.8−2.9 %).

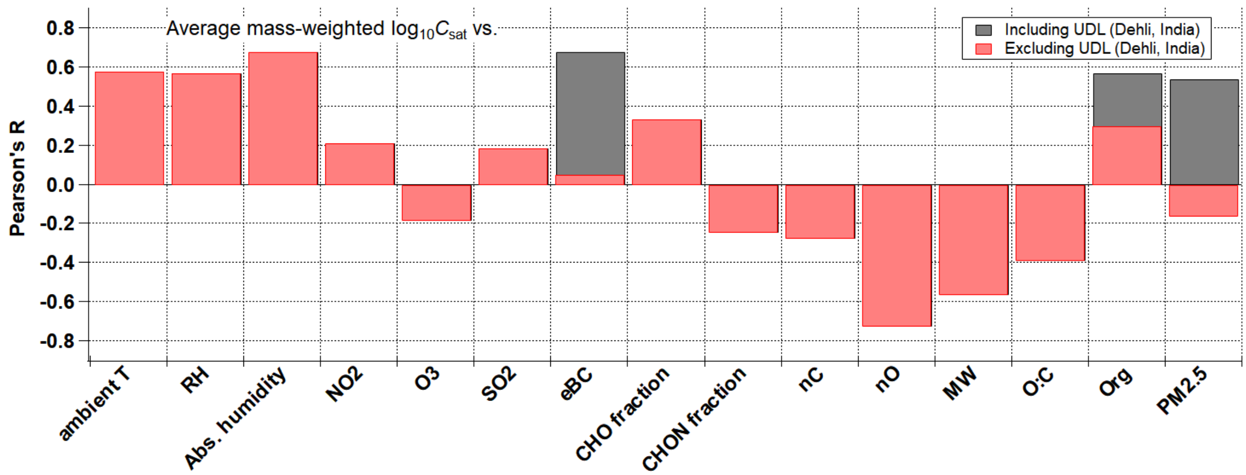

Figure S5. Correlations of campaign-average mass weighted $\log_{10}C_{sat}$ values vs. other parameters. Pearson's R values including and excluding UDL (Dehli, India) data point for eBC, Org, and $PM_{2.5}$ are in gray bars and red bars, respectively, due to their extremely high levels at UDL (see Table S1). Org and $PM_{2.5}$ data were total non-refractory mass concentration from a high-resolution time-of-flight aerosol mass spectrometer (HR-ToF-AMS, Aerodyne Research Inc.) or an aerosol chemical speciation monitor (ACSM, Aerodyne Research Inc.).

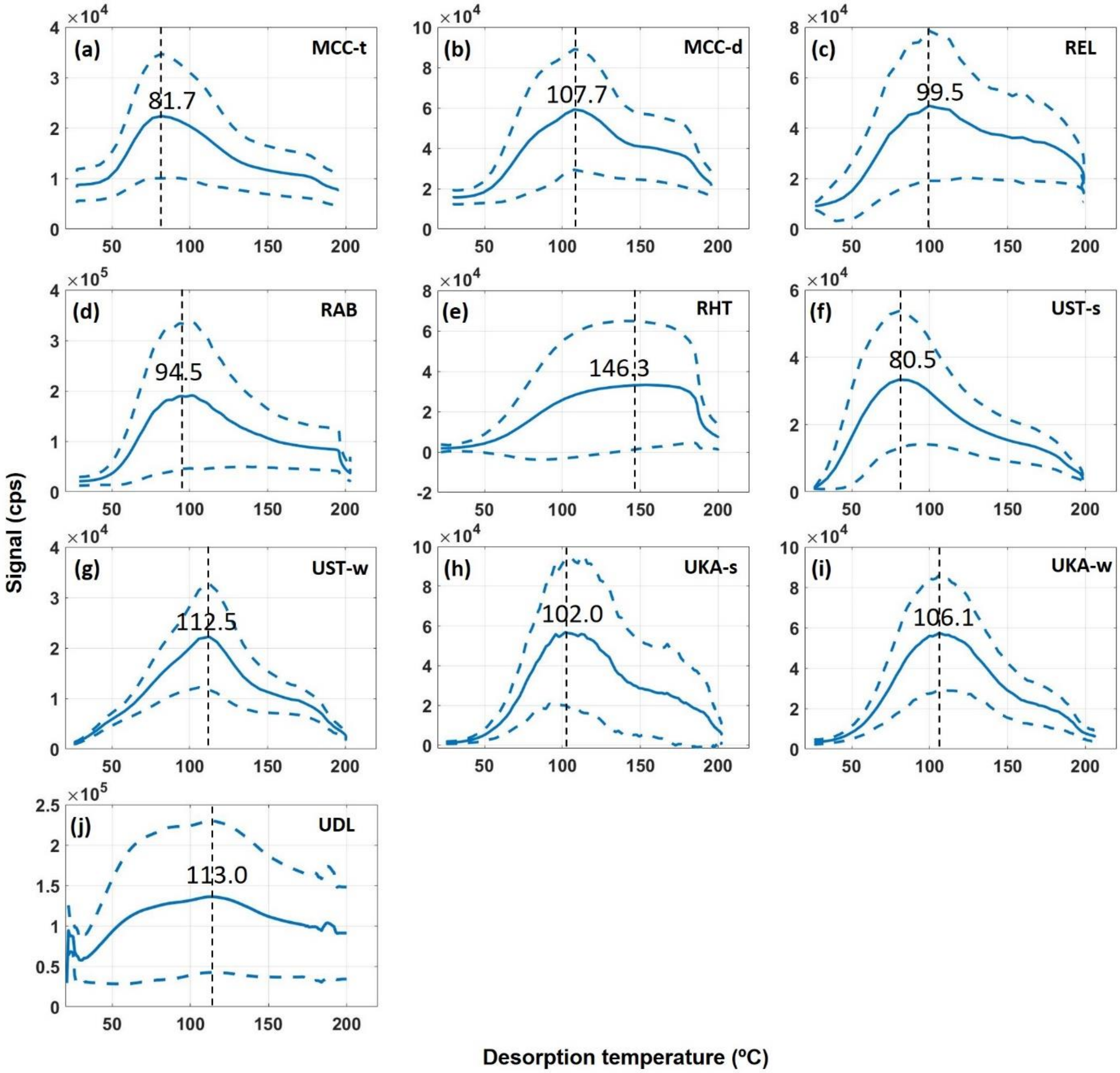

60 **Figure S6.** Campaign-average sum thermograms of CHOX compounds for MCC-t (a), MCC-d (b), REL (c), RAB (d), RHT (e), UST-s (f), UST-w (g), UKA-s (h), UKA-w (i), and UDL (j). Dashed blue lines represent ±1 standard deviation and dashed black lines indicate the sumT_{max} values.

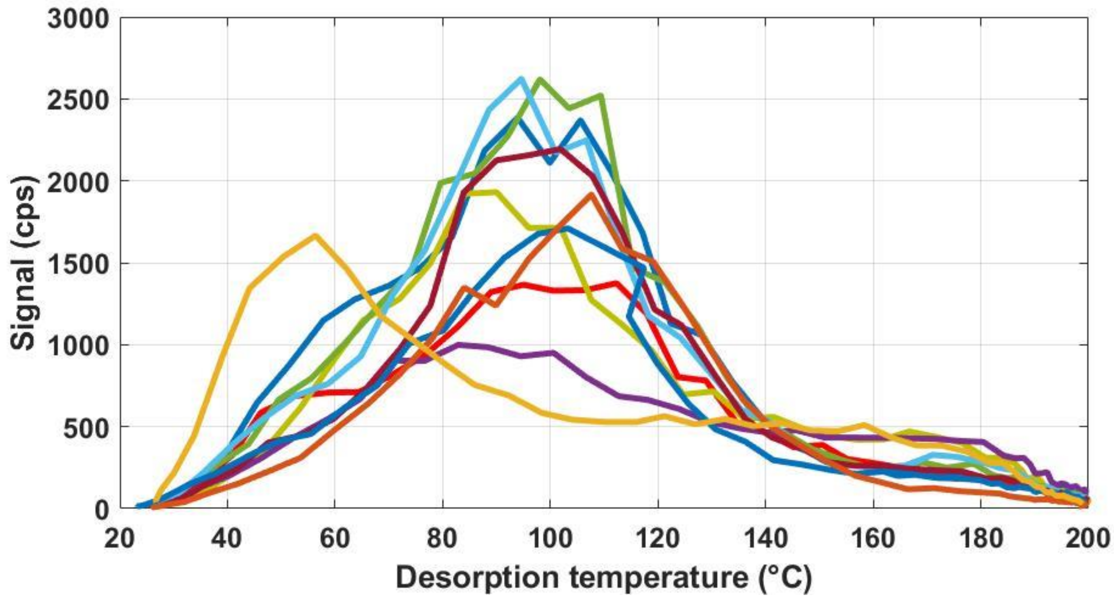

Figure S7. Thermograms of $C_6H_{10}O_5$ compound during the whole campaign in winter Stuttgart (UST-w).

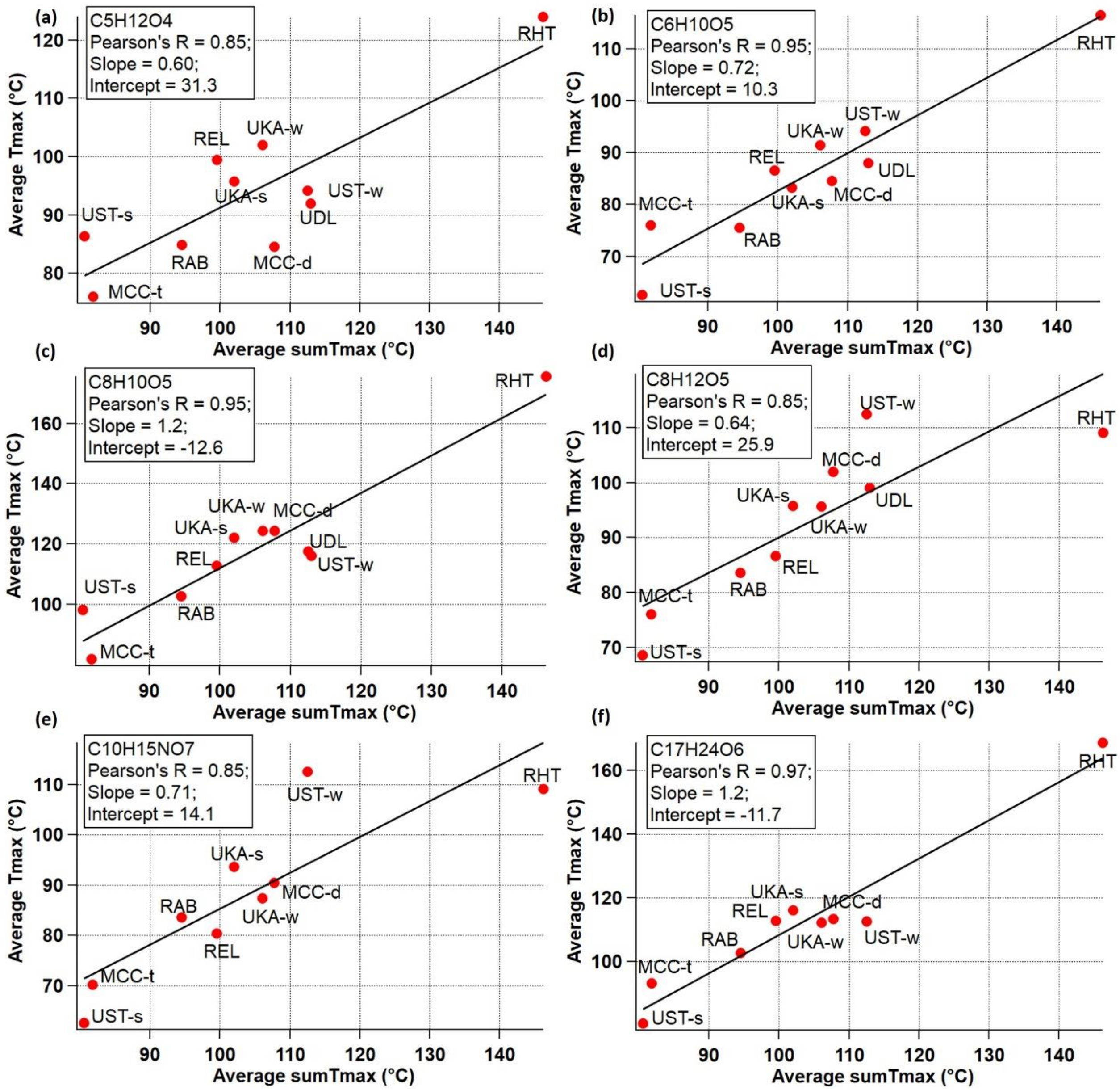

Figure S8. Campaign-average T_{max} values for $C_5H_{12}O_4$ (a), $C_6H_{10}O_5$ (b), $C_8H_{10}O_5$ (c), $C_8H_{12}O_5$ (d), $C_{10}H_{15}NO_7$ (e), and $C_{17}H_{24}O_6$ (f) vs. the corresponding campaign-average sumT_{max} values.

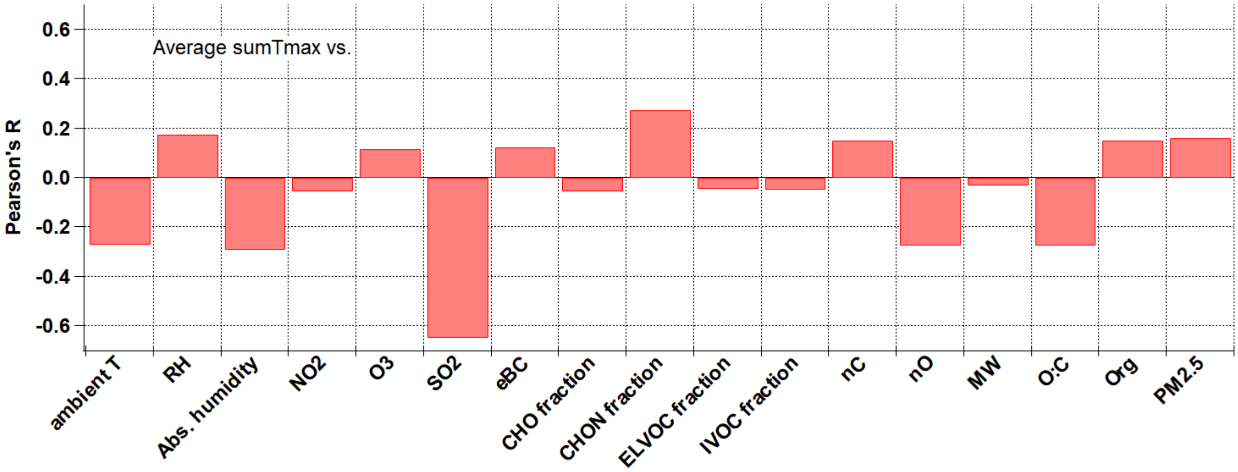

Figure S9. Correlations of campaign-average sumT_{max} values vs. other parameters. Org and $PM_{2.5}$ data were total non-refractory mass concentration from a high-resolution time-of-flight aerosol mass spectrometer (HR-ToF-AMS, Aerodyne Research Inc.) or an aerosol chemical speciation monitor (ACSM, Aerodyne Research Inc.). The negative correlation with SO_2 (Pearson's R: -0.67) could be artificial as SO_2 would not react/condense directly onto aerosol particles and also less SO_2 data points were available for this correlation (see also Table S1). Levels of sulfur-containing organics (CHOS and CHONS) and non-refractory particulate sulfate show no correlations with sumT_{max} values as well.

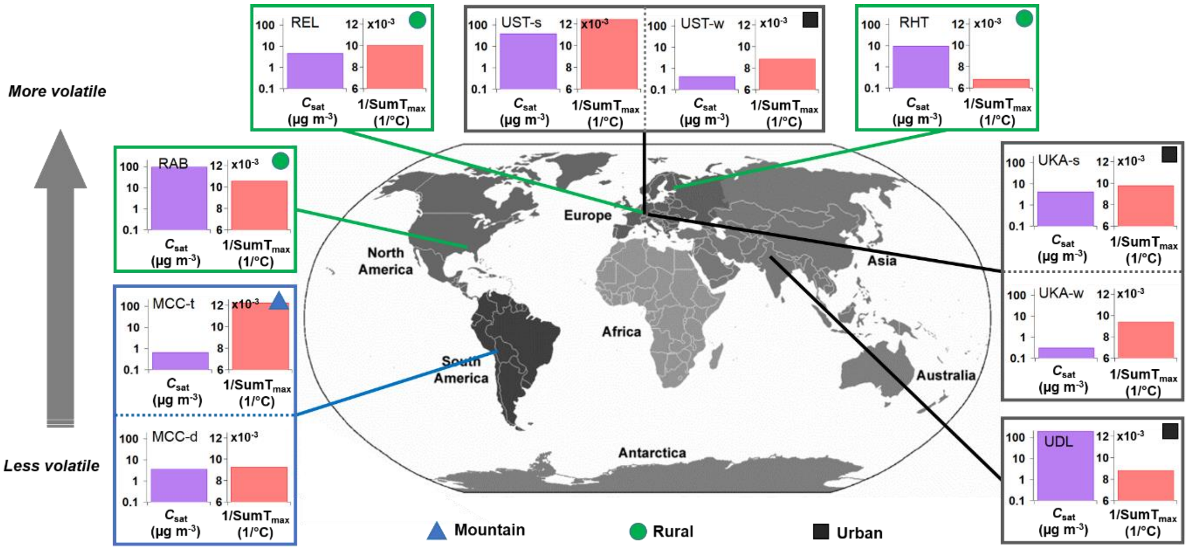

Figure S10. Overview of the comparison of the average C_{sat} (T) (i.e, molecular composition-derived volatility) with the sumT_{max} (i.e., thermal desorption-derived volatility) for different locations and seasons (Mountain sites in triangles, Rural sites in circles, and Urban sites in squares).

References

Daumit, K. E., Kessler, S. H., and Kroll, J. H.: Average chemical properties and potential formation pathways of highly oxidized organic aerosol, Faraday Discuss, 165, 181-202, https://doi.org/10.1039/C3FD00045A, 2013.

Donahue, N. M., Epstein, S. A., Pandis, S. N., and Robinson, A. L.: A two-dimensional volatility basis set: 1. organic-aerosol mixing thermodynamics, Atmos Chem Phys, 11, 3303–3318, https://doi.org/10.5194/acp-11-3303-2011, 2011.

Isaacman-VanWertz, G., and Aumont, B.: Impact of organic molecular structure on the estimation of atmospherically relevant physicochemical parameters, Atmos Chem Phys, 21, 6541–6563, https://doi.org/10.5194/acp-21-6541-2021, 2021.

Li, Y., Pöschl, U., and Shiraiwa, M.: Molecular corridors and parameterizations of volatility in the chemical evolution of organic aerosols, Atmos Chem Phys, 16, 3327–3344, https://doi.org/10.5194/acp-16-3327-2016, 2016.

Lopez-Hilfiker, F. D., Mohr, C., Ehn, M., Rubach, F., Kleist, E., Wildt, J., Mentel, T. F., Lutz, A., Hallquist, M., Worsnop, D., and Thornton, J. A.: A novel method for online analysis of gas and particle composition: description and evaluation of a Filter Inlet for Gases and AEROsols (FIGAERO), Atmos Meas Tech, 7, 983−1001, https://doi.org/10.5194/amt-7-983-2014, 2014.